Multichromophoric Cyclodextrins. 6. Investigation of Excitation Energy Hopping by Monte-Carlo Simulations and Time-Resolved Fluorescence Anisotropy

Mário N. Berberan-Santos,*,† Patricia Choppinet,‡,§ Aleksandre Fedorov,† Ludovic Jullien,⊥ and Bernard Valeur*,‡,§

Contribution from Centro de Química-Física Molecular, Instituto Superior Técnico, 1049-001 Lisboa, Portugal, Laboratoire de Photophysique et Photochimie Supramoléculaires et Macromoléculaires, Ecole Normale Supérieure de Cachan (CNRS UMR 8531), 61 Avenue du Président Wilson, 94235 Cachan Cedex, France, Laboratoire de Chimie Générale, Conservatoire National des Arts et Métiers, 292 rue Saint-Martin, 75003 Paris, France, and Département de Chimie, Ecole Normale Supérieure (CNRS URA 1679), 24 rue Lhomond, 75005 Paris, France

Received October 13, 1998

Abstract: Excitation energy transport in several β-cyclodextrins containing seven appended chromophores was studied theoretically and experimentally by steady-state and time-resolved fluorescence anisotropy. The absorption spectra compared to those of reference chromophores did not reveal significant interactions between the chromophores in the ground state, thus allowing us to assume a very weak coupling regime for energy transfer. The measured long time anisotropies were found to be in all cases close to one-seventh of the fundamental anisotropy, showing that the chromophores are randomly oriented. A realistic model in which the chromophores are in fixed positions but randomly oriented was developed to interpret the steady-state and time-resolved emission anisotropy data. A Monte-Carlo simulation based on the appropriate master equation allowed the calculation of the theoretical anisotropy decay in terms of reduced variables and parameters. The decay contains a wide spectrum of rate constants. A good fit to the experimental decays was obtained. Moreover, the nearest-neighbor distance recovered from the anisotropy and the steady-state anisotropy for all cyclodextrins (5−7 Å in all cases) are compatible with the nearest-neighbor distances expected from molecular modeling, which confirms the validity of the theoretical model.

Introduction

Investigations of excitation energy transport among chromophores are of major interest to understand how nature harvests sunlight.[1,2] In addition, energy transport occurs not only in antennae pigments of photosynthetic units, but also in light-harvesting polymers[3,4] and in antenna-based photomolecular devices.[5] As compared to chromophores assemblies in infinite domains,[6] the case where the number of chromophores is small and fixed (except bichromophoric systems) has not received much experimental and theoretical attention so far, namely owing to the fact that the synthesis of systems containing a limited number of chromophores in well-defined positions is very demanding. Moreover, when the chromophores are close to each other, attention should be paid to the mechanism of transfer, which might not be unique.

β-Cyclodextrins containing seven appended chromophores are good models for the study of excitation energy transport involving a limited number of excitable species with defined positions.[7−12] It is worth noting that the circular arrangement of the chromophores is reminiscent of the light harvesting complex of photosynthetic bacteria (LH2).[13] In a previous paper of this series,[11] we developed a simple theoretical model involving a unique rate constant for energy hopping, supposed to occur only between randomly oriented nearest neighbors. The overall fluorescence anisotropy was found to be a triple exponential decay with equal amplitudes, plus a constant term

† Instituto Superior Técnico.
‡ Ecole Normale Supérieure (Cachan).
§ Conservatoire National des Arts et Métiers.
⊥ Ecole Normale Supérieure (Paris).

(1) *Antennas and Reaction Centers in Photosynthetic Bacteria*; Michel-Beyerle, M. E., Ed.; Springer-Verlag: Berlin, 1985.
(2) *The Photosynthetic Bacterial Reaction Center—Structure and Dynamics*; Breton, J., Vermeglio, H., Eds.; Plenum Press: New York, 1988.
(3) Guillet, J. E. *Polymer Photophysics and Photochemistry*; Cambridge University Press: Cambridge, U.K., 1985.
(4) Webber, S. E. *Chem. Rev.* **1990**, *90*, 1469.
(5) Balzani, V.; Scandola, F. *Supramolecular Photochemistry*; Horwood: New York, 1990.
(6) Bauman, J.; Fayer, M. D. *J. Chem. Phys.* **1986**, *85*, 4087−4107 and references therein.
(7) Berberan-Santos, M. N.; Canceill, J.; Brochon, J. C.; Jullien, L.; Lehn, J. M.; Pouget, J.; Tauc, P.; Valeur, B. *J. Am. Chem. Soc.* **1992**, *114*, 6427−6436.
(8) Berberan-Santos, M. N.; Pouget, J.; Valeur, B.; Canceill, J.; Jullien, L.; Lehn, J.-M. *J. Phys. Chem.* **1993**, *97*, 11376−11379.
(9) Gravett, D. M.; J. Guillet, J. *J. Am. Chem. Soc.* **1993**, *115*, 5970−5974.
(10) Jullien, L.; Canceill, J.; Valeur, B.; Bardez, E.; Lehn, J.-M. *Angew. Chem., Int. Ed. Engl.* **1994**, *33*, 2438−2439.
(11) Berberan-Santos, M. N.; Canceill, J.; Gratton, G.; Jullien, L.; Lehn, J.-M.; Peter So, P.; Sutin, J.; Valeur, B. *J. Phys. Chem.* **1996**, *100*, 15−20.
(12) Jullien, L.; Canceill, J.; Valeur, B.; Bardez, E.; Lefèvre, J. P.; Lehn, J.-M.; Marchi-Artzner, V.; Pansu, R. *J. Am. Chem. Soc.* **1996**, *118*, 5432−5442.
(13) McDermott, G.; Prince, S. M.; Freer, A. A.; Hawthornthwaite-Lawless, Papiz, M. Z.; Cogdell, R. J.; Isaacs, N. W. *Nature* **1995**, *374*, 517−521. Hu, X.; Schulten, K. *Physics Today* **1997** (August), 28−34. Van Grondelle, R.; Monshouwer, R.; Valkunas, L. *Ber. Bunsen-Ges. Phys. Chem.* **1996**, *100*, 1950−1957. Pullerits, T.; Sundström, V. *Acc. Chem. Res.* **1996**, *29*, 381−389.

10.1021/ja983601n CCC: $18.00
Published on Web 03/03/1999

Scheme 1

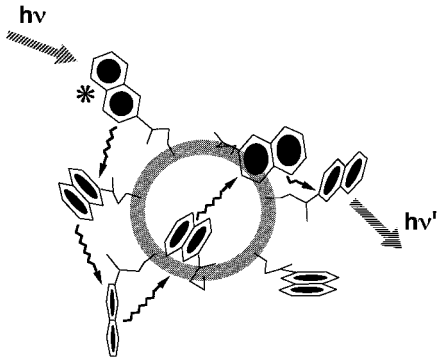

that is one-seventh of the fundamental anisotropy r_0. Steady-state and frequency-domain fluorescence anisotropy experiments carried out on a particular cyclodextrin were in good agreement with a long-time leveling-off of the emission anisotropy at $r_0/7$, thus demonstrating that there is no preferred mutual orientation between the chromophores. The flexibility of the link between the chromophores and the cyclodextrin backbone explain such a random relative orientation. Regarding the dynamics of energy hopping, the difference between the experimental and theoretical anisotropy decay curves was explained by the crude approximations made in the model. In particular, the distributions of distances and mutual orientations of the chromophores were not taken into account.

In the present work, the dynamics of energy hopping was investigated from a completely new point of view much closer to the reality, i.e., with a distribution of rate constants in mind (as suggested by Scheme 1, which illustrates the excitation energy hopping process). Considering the difficulty of the theoretical approach, we performed Monte-Carlo simulations, and the results were used to look for the consistency with experimental data of time-resolved fluorescence anisotropy obtained by the single photon-timing technique. In this investigation, several multichromophoric cyclodextrins were studied. Their chemical structures are shown in Figure 1.

Theory

Mechanism of Transfer. Before designing a model for energy transport among chromophores in a circular arrangement, it is necessary to discuss the possible mechanisms of transfer that are likely to be involved in the multichromophoric cyclodextrins under study. Owing to the flexibility of the link between the chromophores and the cyclodextrin backbone, the interchromophoric distance can be quite short (<10 Å) in several conformations. Therefore, we must examine the relative contribution of Coulombic and short-range interactions.

A careful comparison of the absorption spectra of the labeled cyclodextrins and that of the reference chromophore, NAEt or NAGlu, provides information on possible short-range interactions and especially excitonic coupling. The solubility of CD7-(3) in an ethanol−methanol (9:1) mixture (used for emission anisotropy experiments) was sufficient to determine the molar absorption coefficient. Its wavelength dependence for CD7(3) was found to be very close to that of the reference chromophore NAGlu multiplied by seven in the 220−350 nm range. Therefore, the absence of significant shift and hypo- or hyperchromic effect precludes the existence of significant interaction in the ground state. Unfortunately, such an absolute comparison was not possible with the other cyclodextrins because of the lack of sufficient solubility for accurate determination of the molar absorption coefficients. Nevertheless,

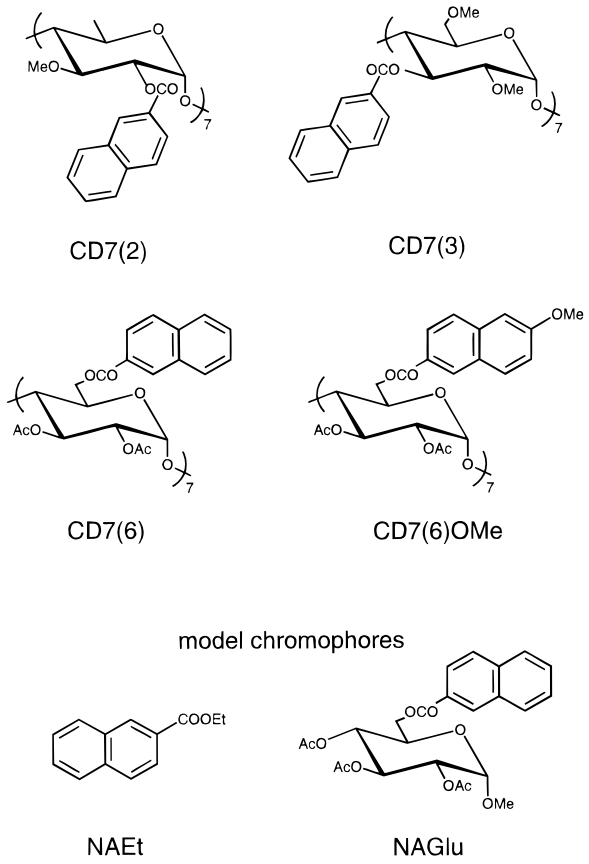

Figure 1. Chemical structure of the multichromophoric cyclodextrins and the relevant model chromophores NAEt and NAGlu.

relative comparison of the absorption spectra could be done by normalization of the spectra at 320 nm. In all cases, the discrepancies between the absorption spectra of the labeled cyclodextrins and those of the relevant reference chromophores were found to be less than 10%. Excitonic coupling can thus be safely ignored.

Resonance energy transfer can then occur according to Coulombic interactions[14] or short-range interactions resulting from interchromophore orbital overlap.[15,16] Regarding the relative contribution of these two processes, it is worth pointing out the observations of Scholes and Ghiggino[17] in the case of naphthalene dimers: they found that at an interchromophoric distance of 4 Å, for instance, the contribution of short-range interactions to the overall calculated electronic coupling is only 17% because the electronic transitions are allowed. In the cyclodextrins labeled with naphthalenic chromophores, we also expect much of the coupling to result from Coulombic interactions rather than short-range interactions.

Let us consider now the Coulombic interactions. At large donor−acceptor separations, the interaction can be well-approximated as point dipole−dipole (Förster theory).[14] But when the donor−acceptor separation approaches the size of the chromophores, the Coulombic term must take into account the shape of the molecular charge distribution. This can be achieved by considering the total excitation as a sum of electrostatic

(14) (a) Förster, Th. *Ann. Phys. (Leipzig)* **1948**, *2*, 55−75. (b) Förster, Th. *Discuss. Faraday Soc.* **1959**, *27*, 7−17; *Modern Quantum Chemistry*; Sinanoglu, O., Ed.; Academic Press: New York, 1965; Part III, pp 93−137.

(15) Dexter, D. L. *J. Chem. Phys.* **1953**, *21*, 836−850.

(16) Speiser, S. *Chem. Rev.* **1996**, *96*, 1953−1976.

(17) Scholes, G. D.; Ghiggino, K. P. *J. Phys. Chem.* **1994**, *98*, 4580−4590.

interactions between point monopoles located at the atoms of the chromophores.[18] The importance of higher order Coulombic interactions can thus be assessed. An interesting application of this method can be found in the work of Fleming et al.[19] dealing with the excitation transfer in the LH2 light harvesting antenna complex of *Rhodobacter sphaeroides*; despite the small interchromophoric separation between the bacteriochlorophyll a molecules, the monopole corrections were found to be only 20% or less.

All these considerations lead us to make the approximation of pure dipole−dipole interaction, i.e., very weak coupling, and to use in the simulations the Förster formula[14b] for the rate constant. The validity of this approximation will be further discussed in view of the results obtained with the various multichromophoric cyclodextrins.

Since we previously showed that there is no preferred orientation between the chromophores,[7,11] our system is relevant to the problem of excitation transport among randomly oriented chromophores in a finite volume under the condition of very weak coupling. This problem was theoretically studied by Ediger and Fayer[20] for randomly distributed chromophores and an isotropic interaction, who found, for a number of chromophores ≤ 3, an exact solution expressed as the Laplace transform of the probability of finding an initially excited chromophore still excited at time *t*. However, for anisotropic interactions and a larger number of chromophores, the developed equations no longer apply. Consequently, we decided to perform Monte-Carlo simulations built upon the appropriate master equation.

Model for Energy Hopping Dynamics. The electronic excitation energy hopping between the seven chromophores of the cyclodextrins studied can be modeled according to the following picture: (i) Chromophores are located at the edges of a regular heptagon, of side R. The nearest-neighbor distance is therefore *R*, while the distances to second and third neighbors are, respectively, 1.802*R* and 2.247*R*. (ii) Orientations of the chromophores are supposed to be uncorrelated and at random. (iii) They are also considered to be frozen. In this way, there will be many different seven-chromophore configurations, each with a particular set of orientations. For each, the possibility of transfer between any pair is allowed for. (iv) The dipole−dipole (Förster) mechanism for transfer of electronic excitation energy is assumed, for which the rate constant for transfer is[14b]

$$k = \frac{3}{2}\frac{\kappa^2}{\tau_0}\left(\frac{\bar{R}_0}{d}\right)^6 \tag{1}$$

where d is the donor−acceptor distance, τ_0 is the fluorescence lifetime, κ^2 is the orientational factor, and $\bar{R}_0$ is the critical (or Förster) radius (computed with $\kappa^2 = {}^2/_3$).

From these assumptions, and for a given set of chromophore orientations (configuration), it follows that the dynamics of incoherent energy hopping is described by the following master equation,[11]

$$\frac{\mathrm{d}\mathbf{P}}{\mathrm{d}t} = \mathbf{K}\mathbf{P} \tag{2}$$

where **P** is the vector of the time-dependent individual excitation probabilities

$$\mathbf{P}(t) = \begin{bmatrix} P_1(t) \\ P_2(t) \\ \ldots \\ P_7(t) \end{bmatrix} \tag{3}$$

and **K** is the matrix of rate constants

$$\mathbf{K} = \begin{bmatrix} -(k_{12}+k_{13}+\ldots+k_{17}) & k_{21} & k_{31} & k_{71} \\ k_{12} & -(k_{12}+k_{13}+\ldots+k_{17}) & k_{32} & k_{72} \\ \ldots & \ldots & \ldots & \ldots \\ k_{17} & \ldots & \ldots & -(k_{71}+k_{72}+\ldots+k_{76}) \end{bmatrix} \tag{4}$$

whose elements are combinations of the i,j pair rate constants ($i, j = 1, 2, \ldots, 7, i \neq j$)

$$k_{ij} = \frac{3}{2}\frac{\kappa_{ij}^2}{\tau_0}\left(\frac{\bar{R}_0}{d_{ji}}\right)^6 \tag{5}$$

where

$$d_{ij} = \alpha_{ij} R \tag{6}$$

and α_{ij} takes the values 1, 1.802, and 2.247 for the first, second, and third nearest-neighbors, respectively. Equation 2 admits an exact solution, given by

$$\mathbf{P}(t) = \exp(\mathbf{K}t)\mathbf{P}_0 \tag{7}$$

where $\mathbf{P}_0$ is the vector of the initial excitation probabilities. To account for the chromophore intrinsic decay, the excitation probability $\mathbf{P}(t)$ should also be multiplied by $\exp(-t/\tau_0)$.[11]

One of the observable quantities that reflects the energy hopping dynamics is the anisotropy of the fluorescence emitted by the excited chromophores. It is well-known that for randomly oriented chromophores the anisotropy of the fluorescence r(t), following excitation of chromophore 1, is to a very good approximation given by[21]

$$r(t) = r_0 P_1(t) \tag{8}$$

where r_0 is the fundamental anisotropy and $P_1(t)$ is the probability that the initially excited chromophore is still excited at time *t*. For long times, this probability attains a limiting value of ${}^1/_7$, corresponding to a maximum spread of the excitation in the seven-chromophore system. The macroscopic probability anisotropy decay $r(t)$, being a sum of contributions from different configurations, can only be obtained as a numerical average

$$r(t) = r_0 \langle P_1(t) \rangle = r_0 P_{\mathrm{in}}(t) \tag{9}$$

where $P_1(t)$ is computed according to eq 7 for each configuration and $P_{\mathrm{in}}(t)$ is the excitation probability of the initially excited chromophore after averaging over configurations. This calculation can be done by Monte-Carlo simulation, as is next described.

Simulation Method. The simulation method is based on the generation of a large number of configurations by the Monte-Carlo method.

(18) Chang, J. C. *J. Chem. Phys.* **1977**, *67*, 3901−3909.

(19) Jimenez, R.; Dikshit, S. N.; Bradforth, S. E.; Fleming, G. R. *J. Phys. Chem.* **1996**, *100*, 6825−6834.

(20) Ediger, M. D.; Fayer, M. D. *J. Chem. Phys.* **1983**, *78*, 2518−2524.

(21) It has been demonstrated in the case of a pair of like molecules that the anisotropy of indirectly excited chromophores is very small (4% of r_0 at time zero) and decays to zero. See: Berberan-Santos, M. N.; Valeur, B *J. Chem. Phys.* **1991**, *95*, 8048−8055.

Once these configurations are obtained, the usual and obvious procedure[4,22,23] is to compute $P_1(t)$ for each configuration, followed by the calculation of the anisotropy decay as a configurational average, according to eq 9. However, the calculation of $P_1(t)$ for each configuration is not direct and implies the determination of the full solution (eq 7) in the following steps:[22,24] (i) calculation of the eigenvalues of **K**; (ii) calculation of a set of eigenvectors of **K**; (iii) calculation of an appropriate set of scalar coefficients.

For the pure hopping case, an alternative and simpler procedure exists, avoiding steps ii and iii mentioned above. In this method, one notes that for each configuration generated each of the seven chromophores is equally likely to be initially excited. It is therefore computationally inefficient to consider only the possibility $P_1(0) = 1$: All seven cases $P_i(0) = 1$ (i = 1, 2, ..., 7) must be taken into account, by means of a pre-averaging procedure. For a given configuration, the rate matrix is $\mathbf{K}^{(c)}$, and

$$\mathbf{P}^{(c)}(t) = \exp(\mathbf{K}^{(c)}t)\mathbf{P}_0 = \mathbf{G}^{(c)}\mathbf{P}_0 \tag{10}$$

In this way, if it is the ith chromophore that is initially excited, the probability that it will remain excited is

$$P_i^{(c)}(t) = G_{ii}^{(c)}(t) \tag{11}$$

and the *average* excitation probability of the initially excited chromophore is, for the configuration

$$P_{\text{in}}^{(c)}(t) = \frac{\sum_i G_{ii}^{(c)}(t)}{7} \tag{12}$$

The numerator of eq 12 is the trace of matrix $\mathbf{G}^{(c)}$ and is therefore base-independent. In this way, if the eigenvalues of matrix $\mathbf{K}^{(c)}$ are $\lambda_1^{(c)}$, $\lambda_2^{(c)}$, ..., $\lambda_7^{(c)}$, eq 12 can be rewritten as

$$P_{\text{in}}^{(c)}(t) = \frac{\sum_i \exp(\lambda_i^{(c)}t)}{7} \tag{13}$$

Finally, the *configurationally averaged* probability is

$$P_{\text{in}}(t) = \frac{\sum_c \sum_i \exp(\lambda_i^{(c)}t)}{7c} \tag{14}$$

where c is the number of configurations. This equation can be rewritten as

$$P_{\text{in}}(t) = \int_{-\infty}^{0} q(\lambda)\exp(\lambda t)\mathrm{d}\lambda \tag{15}$$

where $q(\lambda)$ is the density function of the eigenvalues of **K**. Note that only nonpositive values of λ are to be considered because the probability cannot increase indefinitely and must level off at long times. The anisotropy decay thus becomes

$$r(t) = r_0\int_{-\infty}^{0} q(\lambda)\exp(\lambda t)\mathrm{d}\lambda \tag{16}$$

or, performing the convenient change of variable $k = -\lambda$

$$r(t) = r_0\int_0^{\infty} f(k)\exp(-kt)\mathrm{d}k \tag{17}$$

where $f(k)$ is the density function for positive and zero rate constants. It is important to note that the density function $f(k)$ can be written as

$$f(k) = {}^1/_7\delta(k) + {}^6/_7 f_+(k) \tag{18}$$

where the first term on the right-hand side accounts for the long time limit of the anisotropy and $f_+(k)$ is the density function for *positive* rate constants. In this way, the anisotropy decay takes the form

$$r(t) = \frac{r_0}{7}(1 + 6\int_0^{\infty} f_+(k)\exp(-kt)\mathrm{d}k) \tag{19}$$

and the steady-state anisotropy $\bar{r}$ is calculated by means of the following relation

$$\bar{r} = \frac{\int_0^{\infty} r(t)I(t)\mathrm{d}t}{\int_0^{\infty} I(t)\mathrm{d}t} \tag{20}$$

where $I(t)$ represents the total intensity decay assumed to be a single exponential with time constant τ_0 (intrinsic lifetime of the chromophores). Hence

$$\frac{\bar{r}}{r_0} = \frac{1}{7}\left(1 + 6\int_0^{\infty}\frac{f_+(k)}{1 + k\tau_0}\mathrm{d}k\right) \tag{21}$$

In order to obtain results with maximum generality, and in particular for Monte-Carlo simulations, equations are rewritten in terms of dimensionless parameters. The reduced time T is thus defined

$$T = \frac{3}{2}\left(\frac{\bar{R}_0}{R}\right)^6\left(\frac{t}{\tau_0}\right) = At \tag{22}$$

and the anisotropy decay becomes

$$r(T) = \frac{r_0}{7}(1 + 6\int_0^{\infty} F_+(K)\exp(-KT)\mathrm{d}K) \tag{23}$$

where $F_+(K)$ is the density function of the dimensionless rate constant $K = k/A$. The steady-state anisotropy also becomes

$$\frac{\bar{r}}{r_0} = \frac{1}{7}\left(1 + 6\int_0^{\infty}\frac{F_+(K)}{1 + KA\tau_0}\mathrm{d}K\right) \tag{24}$$

It is also convenient to define a reduced anisotropy $r_{\text{red}}(T)$

$$r_{\text{red}}(T) = \frac{1}{6}\left(7\frac{r(T)}{r_0} - 1\right) \tag{25}$$

Results and Discussion

Monte-Carlo Simulation. A maximum of 200 000 configurations were generated. The reduced anisotropy obtained and the corresponding distribution of rate constants are shown in Figures 2 and 3, respectively. The observed distribution of rate constants covers a very wide dynamic range and is continuous, implying that the anisotropy decay cannot be represented by a sum of a few exponentials. The function $F_+(K)$ is zero at the origin, $F_+(0) = 0$. On the other hand, the function $F_+(K)$ does

(22) Riehl, J. P. *J. Phys. Chem.* **1985**, *89*, 3203−3206.
(23) Finger, K. U.; Marcus, A. H.; Fayer, M. D. *J. Chem. Phys.* **1994**, *100*, 271−286.
(24) Berberan-Santos, M. N.; Martinho, J. M. G. *J. Chem. Educ.* **1990**, *67*, 375−379.

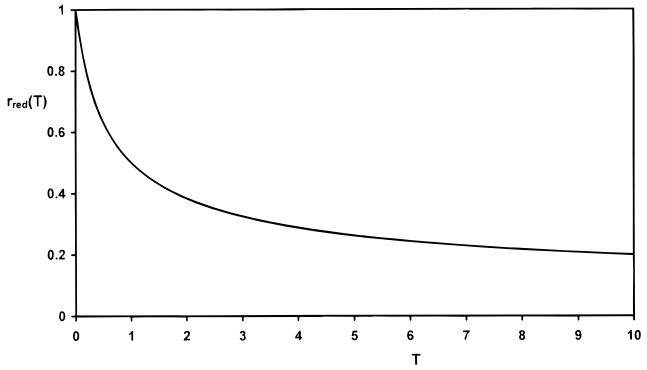

Figure 2. Reduced anisotropy decay $r_{red}(T)$ obtained from Monte-Carlo simulation.

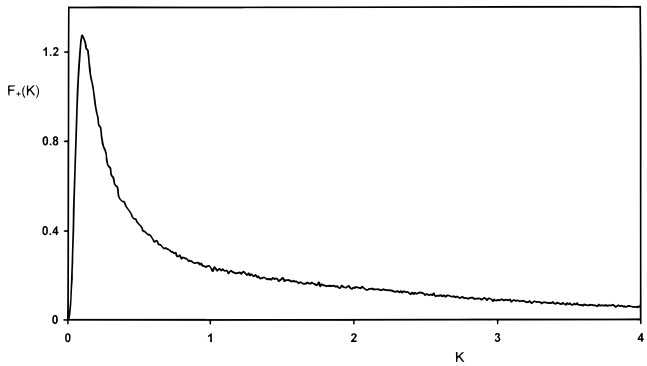

Figure 3. Density function $F_+(K)$ for positive dimensionless rate constants.

not decrease asymptotically toward zero as K goes to infinity, as it may appear from Figure 3. In fact, there is a maximum value of K, corresponding to one of the eigenvalues of an extreme configuration. While this value was not established exactly, it is estimated that $K_{max} \approx 10$. From the obtained distribution, the average rate constant, $\bar{K} = \int_0^\infty K F_+(K) \mathrm{d}K$, can be computed and equals 1.67.

The shape of the obtained curve can be interpreted as follows: low rates have a relatively small probability of occurrence because each chromophore is surrounded by six others, and therefore, it is unlikely that all will have unfavorable orientations for transfer. On the other hand, the relatively wide range of values after the maximum reflects the various possible combinations of orientations for the six pairs. Note that the above qualitative discussion applies regardless the value of $\bar{R}_0$. It is valid even for very small critical radii. If $\bar{R}_0 \ll R$, no significant transfer will of course occur, because the intrinsic decay of the chromophore will usually be much faster. However, if the intrinsic lifetime is supposed to be very long, it is seen that energy transfer can occur, albeit very slowly, and according to the same distribution function for (dimensionless) rates.

In Figure 4, the steady-state anisotropy is shown as a function of $\bar{R}_0/R$. For $\bar{R}_0/R < 0.5$, essentially no hopping is observed; for $\bar{R}_0/R > 2$, complete excitation redistribution over the seven chromophores is reached for times much smaller than the excited-state lifetime.

It is of interest to obtain simple relations for $r_{red}(T)$, for $\bar{r}(\bar{R}_0/R)$, and for $F_+(K)$. The shape of this last function suggests that it could be fitted by a sum of exponentials

$$F_+(K) = \sum_i G_i \exp(-T_i' K) \tag{26}$$

which is in fact only a particular case of

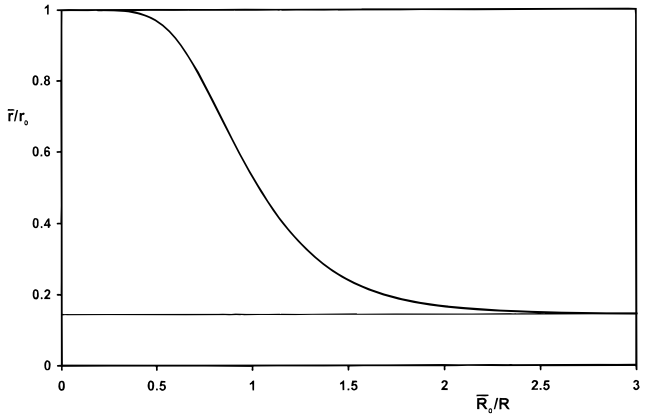

Figure 4. Theoretical steady-state anisotropy as a function of $\bar{R}_0/R$.

$$F_+(K) = \int_0^\infty G(T') \exp(-T'K) \mathrm{d}T' \tag{27}$$

where $G(T')$ is the inverse Laplace transform of $F_+(K)$. This function is, in turn, the inverse Laplace transform of $r_{red}(T)$, as follows from eqs 23 and 25 (see Scheme 2).

In this way, the reduced anisotropy can be written as a double Laplace transform, starting from $G(T')$

$$r_{red}(T) = \int_0^\infty \int_0^\infty \exp(-KT) \exp(-T'K) G(T') \mathrm{d}T' \mathrm{d}K = \int_0^\infty \frac{G(T')}{T + T'} \mathrm{d}T' \tag{28}$$

The steady-state anisotropy is obtained from eq 29 as

$$\frac{\bar{r}}{r_0} = \frac{1}{7}\left(1 + \frac{6}{A\tau_0}\int_0^\infty \exp\left(\frac{T'}{A\tau_0}\right)\mathrm{Ei}\left(\frac{T'}{A\tau_0}\right) G(T') \mathrm{d}T'\right) \tag{29}$$

where $\mathrm{Ei}(x)$ is the exponential integral function, $\mathrm{Ei}(x) = \int_x^\infty \mathrm{e}^{-u}/u \, \mathrm{d}u$. Equation 29 is therefore an alternative to eq 24.

If eq 26 applies, then $G(T')$ reduces to

$$G(T') = \sum_i G_i \delta(T' - T_i') \tag{30}$$

and the reduced anisotropy becomes

$$r_{red}(T) = \sum_i \frac{G_i}{T + T_i'} \tag{31}$$

The advantage of this equation over a sum of exponentials is that a much smaller number of terms is required for a good fit to the simulated curve, essentially because each term already embodies a distribution of exponentials. Not all Gi and T_i' in eq 31 are free parameters. In fact, at least two conditions should be fulfilled:

$$r_{red}(0) = 1 \Rightarrow \sum_i \frac{G_i}{T_i'} = 1 \tag{32}$$

$$F_+(0) = 0 \Rightarrow \sum_i G_i = 0 \tag{33}$$

In this way, in a fit of eq 31 to the simulated decay with n terms, there will be $2(n-1)$ free parameters. Results of the fit, carried out by the method of least squares, were already satisfactory (residues below experimental error) for a sum of three terms (four fitting parameters). For better accuracy, a sum

Scheme 2

$$r_{red}(T) \underset{\mathcal{L}}{\overset{\mathcal{L}^{-1}}{\rightleftharpoons}} F_+(K) \underset{\mathcal{L}}{\overset{\mathcal{L}^{-1}}{\rightleftharpoons}} G(T')$$

Table 1. Best-Fit Parameters of the Simulated Decay of the Reduced Anisotropy[a]

coefficient	value	coefficient	value
G_1	0.415 685	G_3	−2064.425
T_1'	0.505 293	T_3'	14.417 16
G_2	1646.422	G_4	417.5875
T_2'	14.136 54	T_4'	15.521 45

[a] The numerical coefficients of eq 31 were obtained from a least-squares fit with four terms in the interval $T \in [0, 10]$. Only six of the parameters were free, owing to eqs 32 and 33.

Table 2. Experimental Steady-state Anisotropies (Excitation Wavelength 334 nm, Except for CD7(6)OMe, for Which the Excitation Wavelength was 309 nm), as Well as Recovered $\bar{R}_0/R$ Values (from Eq 34), Critical Radii for Transfer, and Recovered Nearest-Neighbor Distances[a]

compd	$\bar{r}$	$\bar{r}/r_0$	$\bar{R}_0/R$	$\bar{R}_0$/Å	R/Å
NAEt	0.342				
NAGlu	0.334				
CD7(2)	0.053	0.16	2.1−2.3	15	7
CD7(3)	0.051	0.15	2.3−2.6	14	6
CD7(6)	0.050	0.15	2.4−2.9	14	5−6
CD7(6)OMe	0.070	0.21	1.6	10	6

[a] The calculated nearest-neighbor distances are estimated to have an uncertainty of ±1 Å.

of four terms was used, and the corresponding coefficients are given in Table 1.

The steady-state anisotropy can also be explicitly computed from eq 31. One obtains

$$\frac{\bar{r}}{r_0} = \frac{1}{7}\left[1 + \frac{6}{A\tau_0}\sum_i G_i \exp\left(\frac{T_i'}{A\tau_0}\right)\mathrm{Ei}\left(\frac{T_i'}{A\tau_0}\right)\right] \qquad (34)$$

Steady-State and Time-Resolved Fluorescence Anisotropy. Excitation polarization spectra of the cyclodextrins were measured in an ethanol−methanol (9:1) rigid glass at 100 K so that no depolarization of fluorescence arises from local motions of the chromophores. Some of the results were previously reported.[7] Calculation of $\bar{r}/r_0$ was performed for the 0−0 transition (334 nm), using for r_0 the value of the reference compounds (NAEt or NAGlu) at the same excitation wavelength or, for CD7(6)OMe, for which data from the reference compound was not available, the recovered initial anisotropy from the experimental anisotropy decay (excitation wavelength 309 nm). Experimental results, as well as recovered $\bar{R}_0/R$ values (from eq 34; see also Figure 4) are given in Table 2. It is seen that almost identical values, within experimental error, are obtained for all compounds. In particular, CD7(6)OMe, mainly on account of the smaller critical radius, has a higher steady-state anisotropy, but nevertheless gives the same nearest-neighbor distance. The obtained distances compare well with those expected from molecular modeling.

Time-resolved anisotropy decays were also recorded for the above compounds under the same conditions. The measured long time anisotropies r_∞ are in all cases equal to one-seventh of the initial values r_0 (fundamental anisotropy) within experimental error, thus confirming the previously published conclusion that chromophores are randomly oriented.[7,11] The decay curve for CD7(6) is shown in Figure 5. Given that for the time scale used (18.4 ps/channel) the pulse width (ca. 40 ps)

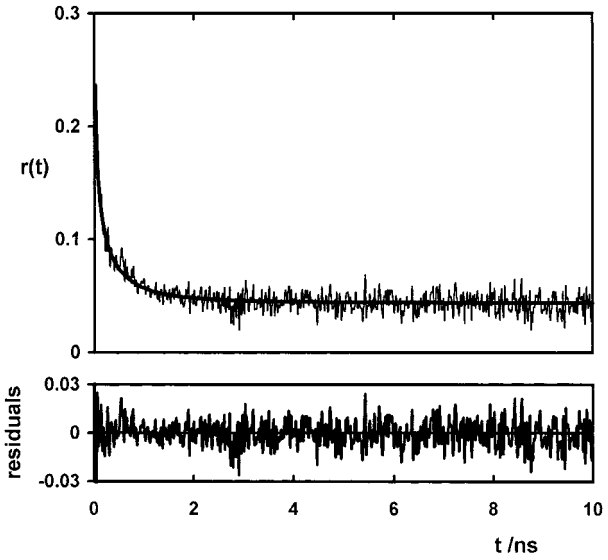

Figure 5. Anisotropy decay of CD7(6) in an ethanol−methanol (9:1) rigid glass at 100 K. Time scale is 18.4 ps/channel. Excitation wavelength was 309 nm, and emission wavelength was 370 nm. For the sake of clarity, only the first half of the decay is shown. It is seen that the long-time limit is already attained 3 ns after the excitation.

Table 3. Recovered Fundamental Anisotropies r_0 and Nearest-Neighbor Distances R from a Fit of Eq 31 to the Time-Resolved Anisotropy Decays[a]

compd	r_∞[b]	r_0	A/ns^{-1}	τ_0/ns	$\bar{R}_0$/Å	$\bar{R}$/Å	$\bar{k}$/ns^{-1}
NAEt		0.262[e]					
NAGlu		0.257[e]					
CD7(2)	0.043[c]	0.299	6.80	15.5	15	7	11.4
CD7(3)	0.042[c]	0.294	11.2	14.9	14	6	18.7
CD7(6)	0.042[c]	0.291	11.7	14.9	14	6	19.5
CD7(6)OMe	0.048[d]	0.339	2.61	10	10	7	4.4

[a] The calculated nearest-neighbor distances are estimated to have an uncertainty of ±1 Å. $\bar{k}$ is the average rate constant (1.67A) (see text). [b] Limiting anisotropy (value at t_∞) [c] Value determined from the plateau at long times. [d] Value determined by curve fitting. [e] Experimental steady-state value.

corresponds to two channels only, the anisotropy decay is here directly reconstructed from the vertically and horizontally polarized decays, without deconvolution. Least-squares analysis was then directly carried out on the anisotropy decays using the following equation, which results from a combination of eqs 22, 25, and 31, together with the values of G_i and T_i' given in Table 1

$$r(t) = \frac{r_0}{7}\left(1 + 6\sum_i \frac{G_i}{At + T_i'}\right) \qquad (35)$$

where

$$A = \frac{3}{2}\frac{1}{\tau_0}\left(\frac{\bar{R}_0}{R}\right)^6$$

The best-fit parameters r_0 and A are given in Table 3. The nearest-neighbor distance R can then be calculated from A, $\bar{R}_0$, and τ_0; the obtained values are similar to those recovered from the steady-state. Some of the fundamental anisotropies recovered are slightly higher than those of the model compounds. Analysis of the decays with those anisotropies fixed at the model compounds values yields nearest-neighbor distances which differ from previous ones by less than 1 Å. An example of recovered distribution of rate constants is shown in Figure 6 for CD7(6).

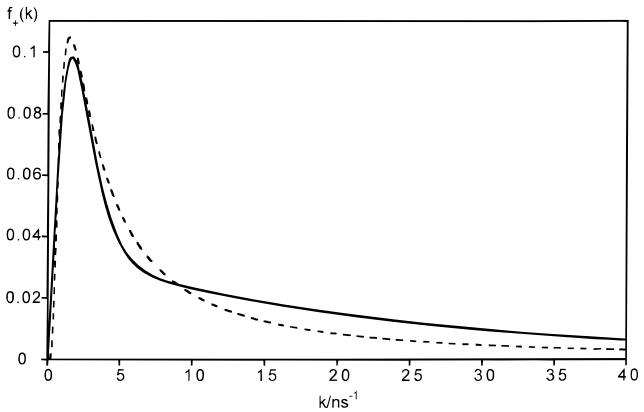

Figure 6. Recovered distribution of rate constants for CD7(6) (solid line). The recovered distribution from the best fit of $r_{red}(t)$ with a stretched exponential [$\exp(-\alpha t^{\beta})$] is shown for comparison (broken line); the exponent β was found to be close to $^1/_2$.

A wide dynamical range is apparent, with an average reciprocal rate constant of 51 ps and a reciprocal rate constant at the maximum of 480 ps.

It should be noted that the experimental steady-state anisotropy values are slightly higher than one-seventh of the corresponding fundamental anisotropies, which results from the fact that the anisotropy decay is not instantaneous. Calculation of the steady-state anisotropies based on the time-resolved data yields results identical (within experimental error) to the experimental ones.

Comparison between CD7(6) and CD7(6)OMe whose structures differ only by the additional methoxy substituent on the naphthalene moiety of the latter is of great interest. Considering the position of this substituent (see Figure 1), no significant difference in the spatial arrangement of the chromophores in the cyclodextrin is expected. But this substituent has a strong effect on the photophysical properties of the chromophore. Despite the fact that the excited-state lifetime, quantum yield, and consequently critical Förster radius are quite different from those of the parent compound CD7(6), it is remarkable that the recovered nearest-neighbor distance is the same within experimental error. This further supports the validity of the theoretical model and in particular the assumption of Förster mechanism for energy transfer.

Concluding Remarks

Excitation energy transport in several β-cyclodextrins containing seven appended chromophores was studied theoretically and experimentally. Comparison of the absorption spectra with those of reference chromophores revealed no significant interaction between the chromophores in the ground state. Moreover, the emission anisotropy levels off at long time intervals, and the limiting anisotropies are in all cases close to one-seventh of the fundamental anisotropy, thus confirming that the chromophores are randomly oriented.

These findings allowed us to develop a realistic model of fixed positions but random orientations of the chromophores under the assumption of very weak coupling (Förster mechanism). The possibility of transfer between any pair and not only between nearest neighbors was allowed. A Monte-Carlo simulation based on the appropriate master equation was performed in order to calculate the theoretical anisotropy decay in terms of reduced variables and parameters. This decay contains a wide spectrum of rate constants and was shown to be better represented by a sum of a few hyperbolic terms than by a sum of the same number of exponentials.

A good fit to the experimental anisotropy decays was obtained, and the recovered parameters (fundamental anisotropy and nearest-neighbor distance from the anisotropy decay; nearest-neighbor distance from the steady-state anisotropy) for all cyclodextrins are physically reasonable and coherent. In particular, the nearest-neighbor distances fall in the range 5−7 Å in all cases, which is compatible with the nearest-neighbor distances expected from molecular modeling. These observations confirm the validity of the theoretical model.

In the simulations, only a distribution of orientations was considered and not a distribution of nearest-neighbor distances, as is expected from molecular modeling, because this distribution of distances is not known and could be narrow. Despite this approximation, the fit to the experimental anisotropy decay is very good. This means that the effect of orientation is predominant with respect to that of distance, or that a longer distance with a more favorable orientation is somewhat equivalent—in terms of transfer rate—to a shorter distance with a less favorable orientation.

In the present investigation, we faced the difficult problem of recovering a distribution of rate constants from an emission anisotropy decay curve. This problem is even more difficult than the recovery of lifetime distributions from fluorescence decay curves. When no a priori assumption of the shape of a distribution can be made, the maximum entropy method (MEM)[25] is in principle appropriate. This method—via global analysis of the two polarized components of the emitted fluorescence—failed to recover a distribution resembling that obtained by Monte-Carlo simulation despite that the MEM solution fitted well to the experimental decays. Attempts at fitting with a stretched exponential (which has already been used in various situations to characterize distributions of relaxation times) gave a reasonable agreement with the experimental decays (see Figure 6), but the physical basis of this law is questionable. Finally, the present work emphasizes the utility of Monte-Carlo simulations for the interpretation of experimental anisotropy decays with underlying distributions of rate constants for energy transfer.

Experimental Section

Synthesis. The syntheses of CD7(2), CD7(3), CD7(6), and the model chromophores NAEt and NAGlu were previously described.[7]

CD7(6)OMe was prepared by coupling the 6-methoxy-2-naphthoic acid[26] with the per-2,3-acetyl-β-cyclodextrin[27] with DCC in dry dichloromethane at room temperature in 60% yield:[28] ^{1}H NMR ($CDCl_3$) 8.57 (s, 1H), 8.06 (d, $J = 9$ Hz, 1H), 7.95 (d, $J = 9$ Hz, 1H), 7.78 (d, $J = 9$ Hz, 1H), 7.13 (d, $J = 9$ Hz, 1H), 7.08 (s, 1H), 5.51 (dd $J_{32} = 9.3$ Hz and $J_{34} = 8.8$ Hz, 1H, H(3)), 5.36 (d, $J_{12} = 3.7$ Hz, 1H, H(1)), 4.96 (d, $J_{6a5} = 12.2$ Hz, 1H, H(6a)), 4.88 (dd, $J_{21} = 3.7$ Hz, $J_{23} = 9.3$ Hz, 1H, H(2)), 4.74 (d, $J_{6b5} = 10.0$ Hz, 1H, H(6b)), 4.45 (d, $J_{54} = 9.2$ Hz, 1H, H(5)), 4.00 (dd, $J_{43} = 8.8$ Hz and $J_{45} = 9.2$ Hz, 1H, H(4)), 3.84 (s, 3H), 2.18 (s, 3H), 2.11 (s, 3H); ^{13}C NMR ($CDCl_3$) 170.8, 169.4, 165.9, 159.3, 137.2, 131.1 (2), 127.9, 126.9, 124.7, 119.4, 105.5, 96.7 (C1), 76.5 (C4), 71.0 (C2 and C3), 70.0 (C5), 62.7 (C6), 55.2, 20.9, 20.8. Anal. Calcd for $(C_{22}H_{22}O_9)7{:}2.5H_2O$ (3057.8): C, 60.49; H, 5.24. Found: C, 60.44; H, 5.19. TLC: elution dichloromethane−ethanol 95% (90:10) $R_f = 0.71$.

Spectroscopic Measurements and Calculations. The UV−vis absorption spectra were recorded on a Kontron Uvikon-940 spectrophotometer. Corrected fluorescence spectra were obtained with a SLM 8000 C spectrofluorometer. All solvents used were of spectroscopic grade.

(25) Livesey, A. K.; Brochon, J. C. *Biophys. J.* **1987**, *52*, 693−706.
(26) Jacques, J.; Horeau, A. *Bull. Soc. Chim. Fr.*, **1950**, *17*, 512−520.
(27) Baer, H. H.; Shen, Y.; González, F. S.; Berenguel, A. V.; García, J. I. *Carbohydr. Res.* **1992**, *135*, 129−139.
(28) Jullien, L.; Canceill, J.; Lacombe, L.; Lehn, J.-M. *J. Chem. Soc., Perkin Trans. 2*, **1994**, 989−1002.

Steady-state fluorescence anisotropies defined as $r = (I_{||}-I_{\perp})/(I_{||} + 2I_{\perp})$ (where $I_{||}$ and $I_{\perp}$ are the fluorescence intensities observed with vertically polarized excitation light and vertically and horizontally polarized emissions, respectively) were determined by the G factor method. The low-temperature (100 K) measurement methods of the cyclodextrins in an ethanol−methanol (9:1) rigid glass was previously reported.[7]

Förster critical radii for transfer $\bar{R}_0$ with $\kappa^2 = {}^2/_3$ were evaluated from the following relation

$$\bar{R}_0 = 0.2108[2/3\Phi_0 n^{-4}\int_0^{\infty} I(\lambda)\epsilon(\lambda)\lambda^4 \mathrm{d}\lambda]^{1/6}$$

with $\bar{R}_0$ in Å, where Φ_0 is the fluorescence quantum yield of the reference chromophore, n is the average refractive index of the medium in the wavelength range where spectral overlap is significant, λ is the wavelength in nanometers, $I(\lambda)$ is the normalized fluorescence spectrum, and $\epsilon(\lambda)$ is the molar absorptivity (in $dm^3 \cdot mol^{-1} \cdot cm^{-1}$). The values of $\bar{R}_0$ for CD7(2), CD7(3), and CD7(6) were previously determined.[7] For CD7(6)OMe, the value was calculated using the fluorescence quantum yield of methyl 6-(methoxy)-2-naphthoate. That quantum yield was determined with PPO in undegassed cyclohexane, $\Phi_0 = 0.90$ as the standard and found to be 0.52.

Time-Resolved Fluorescence. Time-resolved picosecond fluorescence intensity decays were obtained by the single-photon timing method with laser excitation. The setup consisted of a mode-locked Coherent Innova 400−10 argon-ion laser that synchronously pumped a cavity dumped Coherent 701−2 dye (rhodamine 6G) laser, delivering 3−4 ps pulses (with ca. 40 nJ/pulse) at a frequency of 3.4 MHz. Intensity decay measurements were made by alternated collection of impulse and decays with the emission polarizer set at the vertical, horizontal, and magic angle positions. Impulse was recorded slightly away from excitation wavelength with a scattering suspension. For the decays, a cutoff filter was used, effectively removing all excitation light. Detection was always done by passing the emission through a depolarizer and then through a Jobin-Yvon H*R*320 monochromator with a grating of 100 lines/mm. The *G* factor of the system is unity, and for the calculation of the anisotropy identical accumulation times were used for both the vertical and the horizontal components, until a total of no less than 20 000 counts at the maximum channel was obtained for the vertical component. A time scale of 18.4 ps/channel was used. The detector employed was a Hamamatsu 2809U-01 microchannel plate photomultiplier. The instrument response function had an effective fwhm of 40 ps.

Acknowledgment. The authors wish to thank Dr. Josette Canceill and Prof. Jean-Marie Lehn for their contribution to the synthesis of the labeled cyclodextrins. Thanks are also due to Dr. Jean-Claude Brochon for his help in the use the maximum entropy method for attempting to recover the distribution of rate constants. Travel grants to M.N.B.S. and B.V. from ICCTI (Portugal)−CNRS (France) joint program are acknowledged. A.F. was supported through an INVOTAN grant (ICCTI, Portugal).

JA983601N